

Temperature Dependence of Air–Water Partitioning of N-Methylated (C1 and C2) Fatty Acid Amides

Milan Bernauer and Vladimír Dohnal*

Department of Physical Chemistry, Institute of Chemical Technology, 166 28 Prague 6, Czech Republic

Air–water partitioning of lower N-methylated fatty acid amides (*N*-methylformamide, *N*-methylacetamide, *N,N*-dimethylformamide, and *N,N*-dimethylacetamide) was examined at several temperatures in the range from (333 to 373) K employing comparative ebulliometry, differential distillation, and the method of limiting (infinite dilution) relative volatility, limiting activity coefficient, Henry's law constant, and air–water partition coefficient. For each amide, the present air–water partitioning data and some other relevant VLE measurements from the literature were combined with existing calorimetric data on respective derivative thermal properties and correlated simultaneously by a suitable model equation. In the entire treatment, precautions were taken to minimize the effect of uncertain vapor pressures of pure amides at lower temperatures. Recommended thermodynamically consistent temperature dependences of the air–water partitioning characteristics were established allowing their reliable extrapolation to lower (ambient) temperatures where low volatility of aqueous amides hinders direct measurements. Furthermore, the performance of three predictive approaches, namely, the modified UNIFAC, the method of Cabani et al. (*J. Solution Chem.* **1981**, *10*, 563–595), and the LFER correlation of Abraham (*Fluid Phase Equilib.* **2007**, *262*, 97–110), to estimate the air–water partitioning of the amides was tested.

Introduction

N-Methylated formamides and acetamides are highly boiling polar liquids exhibiting very good solvency for both organic compounds and inorganic electrolytes. Due to their favorable solvent properties, these amides are produced on a large scale and used extensively in the manufacture of pharmaceuticals, pesticides, fibers, adhesives, and batteries. Besides their practical applications, the amides are also of great theoretical interest. The amide linkage forms an essential part of the backbone of peptides and various proteins, thus playing a central role in biochemistry. N-Alkylated amides (and in particular *N*-methylacetamide) are used to mimic the peptide bond in modeling the behavior of large and complex biomolecules.

Like water, the amides have an extremely high dielectric constant which makes the two, otherwise distinct media, quite compatible. Despite small deviations from Raoult's law, the molecular complexity of the amide–water mixtures appears to be considerable from both interactional and structural points of view, thus presenting continuing research challenges.^{1–6} Because of the practical and theoretical importance, the aqueous solutions of amides have been studied extensively. Among numerous thermodynamic measurements on the amide–water mixtures, those of vapor–liquid equilibria are however relatively scarce and, apart from a few exceptions,^{7–11} also quite uncertain. In particular, lack of reliable experimental information on the air–water partitioning of amides is notable, reflecting probably experimental difficulties associated with low volatility of amides from their aqueous solutions.

In this work, we examine the air–water partitioning for the four lower N-methylated fatty acid amides, namely, *N*-meth-

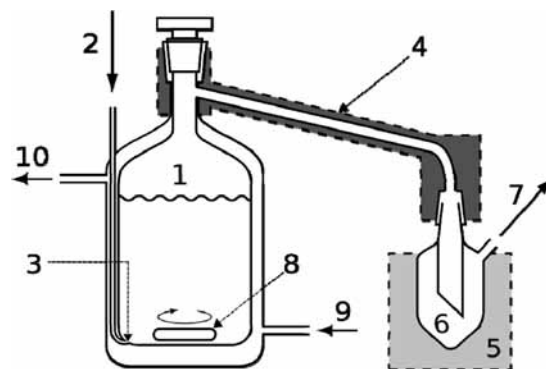


Figure 1. Differential distillation apparatus: 1, equilibrium cell; 2, stripping gas inlet; 3, fritted glass tip; 4, heated transfer line; 5, cold trap; 6, detachable recipient of condensate; 7, stripping gas outlet; 8, magnetic stirrer; 9, input of thermostating water; 10, output of thermostating water.

ylformamide (NMF), *N*-methylacetamide (NMA), *N,N*-dimethylformamide (DMF), and *N,N*-dimethylacetamide (DMA). To cope with the problem of their low volatility, we performed our measurements by suitable techniques at rather elevated temperatures (> 333 K). Combining the present air–water partitioning data and some other relevant VLE measurements from the literature with existing calorimetric data on respective derivative thermal properties and correlating them simultaneously by a suitable model equation, we establish recommended thermodynamically consistent temperature dependences of the air–water partitioning characteristics allowing their reliable extrapolation to lower (ambient) temperatures.

Experimental Section

Materials. *N*-Methylformamide (99.0 %), *N*-methylacetamide (99.5 %), *N,N*-dimethylformamide (99.8 %), and *N,N*-dimethy-

* To whom correspondence should be addressed. E-mail: dohnalv@vscht.cz. Tel.: +420 220 444 297. Fax: +420 220 444 333.

Table 1. Experimental Values of Limiting Relative Volatility α_{12}^{∞} , Henry's Law Constant K_H , Air–Water Partition Coefficient K_{aw} , and Limiting Activity Coefficient γ_1^{∞} for N-Methylated Amides (1) in Water (2) Determined in This Work

T/K	α_{12}^{∞}	K_H/kPa	$10^6 K_{aw}$	γ_1^{∞}	method ^d
NMF					
333.15	0.0255	0.509	3.37	1.37	DDIST
343.15	0.0303	0.944	6.11	1.42	DDIST
353.15	0.0350	1.66	10.5	1.44	DDIST
372.65	0.0500	4.98	30.2	1.65	CIRC
NMA					
333.15	0.0188	0.376	2.49	1.70	DDIST
343.15	0.0235	0.732	4.74	1.78	DDIST
353.15	0.0282	1.34	8.45	1.82	DDIST
DMF					
343.73	0.254	8.13	52.6	1.23	EBU
349.05	0.265	10.6	67.9	1.27	EBU
353.45	0.272	13.0	82.4	1.30	EBU
357.91	0.273	15.6	97.8	1.30	EBU
358.50	0.287	16.8	105	1.36	EBU
363.82	0.286	20.6	127	1.35	EBU
368.38	0.340	29.0	178	1.59	EBU
371.62	0.332	31.9	194	1.54	EBU
372.00	0.359	34.9	212	1.66	EBU
DMA					
343.15	0.132	4.12	26.6	1.27	DDIST
343.51	0.134	4.25	27.5	1.29	CIRC
349.03	0.155	6.21	39.7	1.46	EBU
351.15	0.147	6.42	40.8	1.37	DDIST
353.50	0.186	8.96	56.6	1.72	EBU
353.50	0.194	9.33	59.0	1.79	CIRC
363.87	0.234	16.9	104	2.06	EBU
363.87	0.255	18.4	114	2.24	CIRC
370.86	0.248	23.1	141	2.12	EBU
372.28	0.241	23.7	144	2.05	CIRC

^a CIRC, circulation still method; EBU, comparative ebulliometry; DDIST, differential distillation method.

acetamide (99.5 %) used as solutes were all obtained from Sigma-Aldrich. Their declared purity was verified by gas chromatography using a DB-5 capillary column. Before the measurements, they were dried with 4 Å molecular sieves and stored in the dark. Water used as the solvent was distilled and subsequently treated by a Milli-Q Water Purification System (Millipore, USA).

Apparatus and Procedure. To determine the air–water partitioning, three experimental techniques were employed in this work: comparative ebulliometry (EBU), the method of the circulation still (CIRC), and the differential distillation method (DDIST). The EBU and CIRC are well-established techniques in our laboratory and have been described by us previously:^{12–14} given below is thus only a brief outline supplemented by some details specific to the present application. The DDIST method, which has been newly implemented in this work to cope with a rather low relative volatility of the solutes studied, is described below in detail. The EBU and CIRC methods were used at temperatures from (343 to 373) K where the sufficiently high

water vapor pressure ensures uncompromised performance of the Cottrell pump devices. The DDIST method was applied in the temperature range from (333 to 353) K, the temperature interval being delimited at the lower end by acceptability of the duration of the experiments and at the upper end by circulating water from a thermostat. In the treatment of all VLE data, the vapor phase was considered as an ideal gas since our estimations showed vapor-phase nonideality corrections to be negligible compared to experimental uncertainties.

Comparative Ebulliometry (EBU). The technique consists of measuring ΔT between the boiling temperatures of a dilute solution in a measuring ebulliometer and the pure solvent in a reference ebulliometer under isobaric condition as a function of gravimetrically determined overall composition of the dilute solution x_1^0 . The limiting (infinite dilution) relative volatility α_{12}^{∞} was calculated from the measured limiting slope $(\partial\Delta T/\partial x_1^0)_p^{\infty}$ by means of an explicit equation incorporating corrections for the evaporation ratio f and the vapor phase holdup N_V in the ebulliometer¹³

$$\alpha_{12}^{\infty} = \frac{f + 1 - (d \ln p_2^s/dT)(\partial\Delta T/\partial x_1^0)_p^{\infty}(1 - N_V)}{f + 1 + (d \ln p_2^s/dT)(\partial\Delta T/\partial x_1^0)_p^{\infty}(f + N_V)} \quad (1)$$

The values of the characteristic ebulliometer parameters ($f = 0.06$, $N_V = 0.02$) determined previously¹³ were used for the present calculations.

Circulation Still Method (CIRC). In this method, a VLE circulation still operated at constant pressure is employed to provide samples of the vapor and liquid in equilibrium in the region of high dilution, no measurement of temperature being needed as the boiling temperature of the solution is effectively the same as that of the neat solvent water. Provided the samples are analyzed by a method responding proportionally to the solute concentration, the value of α_{12}^{∞} is obtained from

$$\alpha_{12}^{\infty} = \frac{A_1^G}{A_1^L} \quad (2)$$

where A_1^G and A_1^L are the responses for the samples of equilibrium vapor phase condensate and the corresponding liquid phase, respectively. The aqueous solutions studied in this work (solute mole fraction from 10^{-4} to 10^{-3}) were boiled for extended periods of time, (24 to 30) h, to ensure the generation of truly representative equilibrium samples. The samples were analyzed by gas chromatography using an Agilent 6890 Plus GC and a 0.5 m long stainless steel 1/8" o.d. column packed with Carbowax B coated with 4 % Carbowax 20 M and 0.8 % KOH from Supelco. They were injected by an Agilent 7683 automatic sampler, typically with a dozen replicates each.

Differential Distillation Method (DDIST). This simple old technique¹⁵ is based on one-stage equilibrium flask-to-flask distillation in the course of which just a relatively small amount is distilled off from a batch of a highly dilute solution under study

Table 2. Constants of Vapor Pressure Equations of Pure Amide Solute^a

solute	equation	A	B	C	D	T_c/K	p_c/MPa	range ^b	ref
NMF	Riedel-Planck ^c	63.216	-8851.0	-6.48	2.3916E-18			269 to 721	16
NMA	Wagner ^{d,e}	-14.22421	16.68970	-18.29524	6.18819	718.0	4.98	333 to 443	7
DMF	Wagner ^f	36.48688	-68.67427	62.2708	-229.0057	596.6	5.22	307 to 370	17
DMA	Wagner ^{d,g}	-25.70586	48.84239	-54.42768	41.32778	658.0	4.03	298 to 423	18

^a Vapor pressures of solvent water were obtained from equation given by Wagner and Pruss.¹⁹ ^b K. ^c $\ln(p^s/kPa) = A + B/(T/K) + C \ln(T/K) + D(T/K)^6$. ^d $\ln(p^s/p_c) = (T_c/T)(AF + BF^{1.5} + CF^{2.5} + DF^5)$; $F = 1 - T/T_c$. ^e The parameters were obtained in this work by fitting the original data omitting an apparent outlier data point at 338.15 K. ^f $\ln(p^s/p_c) = (T_c/T)(AF + BF^{1.25} + CF^3 + DF^7)$; $F = 1 - T/T_c$. ^g The parameters were obtained in this work by fitting the original data (the parameter values reported in the cited source are incorrect).

Table 3. Values of Limiting Activity Coefficients γ_1^∞ and Henry's Law Constants K_H for N-Methylated (C1 and C2) Fatty Acid Amides (1) in Water (2) Used in Simultaneous Fits by Equation 6

T/K	$\ln \gamma_1^\infty$	s ($\ln \gamma_1^\infty$)	$\ln(K_H/$ kPa)	$s[\ln(K_H/$ kPa)]	technique ^a	ref
NMF						
303.15	0.110 ^b	0.1	-2.70 ^b	0.1	TENS	9
313.15	0.100 ^b	0.1	-2.25 ^b	0.1	TENS	8
333.15	0.312	0.03	-0.676	0.03	DDIST	this work
343.15	0.347	0.03	-0.058	0.02	DDIST	this work
353.15	0.366	0.03	0.507	0.03	DDIST	this work
372.65	0.500	0.05	1.606	0.03	CIRC	this work
NMA						
333.15	0.383 ^b	0.05	-1.097 ^b	0.05	CIRC	7
353.15	0.507 ^b	0.05	0.208 ^b	0.05	CIRC	7
373.15	0.601 ^b	0.05	1.333 ^b	0.05	CIRC	7
298.15	-1.13 ^c	1	-5.16 ^d	1	TRANS	25
313.15	0.216 ^b	0.05	-2.780 ^b	0.05	TENS	10
333.15	0.528	0.05	-0.979	0.03	DDIST	this work
343.15	0.577	0.05	-0.311	0.03	DDIST	this work
353.15	0.601	0.05	0.290	0.03	DDIST	this work
DMF						
323.15	-0.117	0.2	0.777 ^e	0.2	EBU	26
333.05	0.300	0.2	1.699 ^e	0.2	EBU	26
343.05	0.982	0.5	2.843 ^e	0.2	EBU	26
289.4	-0.545	0.2	-2.010 ^e	0.2	DEWT	27
298	-0.431	0.2	-1.166 ^e	0.2	DEWT	27
307.8	-0.211	0.2	-0.236 ^e	0.2	DEWT	27
317.9	-0.051	0.2	0.549 ^e	0.2	DEWT	27
328.3	0.104	0.2	1.267 ^e	0.2	DEWT	27
338	0.262	0.2	1.895 ^e	0.2	DEWT	27
292	-0.511	0.2	-1.743 ^e	0.2	DEWT	28
308.3	-0.357	0.2	-0.349 ^e	0.2	DEWT	28
318.1	-0.223	0.2	0.389 ^e	0.2	DEWT	28
328.3	0.000	0.2	1.163 ^e	0.2	DEWT	28
337.8	0.095	0.2	1.719 ^e	0.2	DEWT	28
347.4	0.095	0.2	2.147 ^e	0.2	DEWT	28
348.15	0.344	0.05	2.427 ^e	0.05	EBU	29
358.15	0.405	0.05	2.905 ^e	0.05	EBU	29
368.15	0.476	0.05	3.373 ^e	0.05	EBU	29
343.73	0.208	0.05	2.096	0.03	EBU	this work
349.05	0.245	0.1	2.364	0.03	EBU	this work
353.45	0.263	0.05	2.568	0.03	EBU	this work
357.91	0.261	0.05	2.749	0.05	EBU	this work
358.50	0.312	0.05	2.824	0.03	EBU	this work
363.82	0.300	0.1	3.025	0.05	EBU	this work
368.38	0.464	0.05	3.368	0.03	EBU	this work
371.62	0.433	0.05	3.462	0.03	EBU	this work
372.00	0.510	0.05	3.554	0.03	EBU	this work
DMA						
298.15	-1.34 ^c	1	-2.582 ^d	1	TRANS	25
314.3	1.56 ^f	1	1.304 ^g	1	RDIST	30
343	1.47 ^f	1	2.691 ^g	1	RDIST	30
358	1.58 ^f	0.5	3.453 ^g	0.5	RDIST	30
373	1.57 ^f	0.5	4.048 ^g	0.5	RDIST	30
313.15	-0.429 ^b	0.1	-0.849 ^b	0.1	TENS	11
343.15	0.241	0.1	1.415	0.10	DDIST	this work
343.51	0.256	0.1	1.447	0.05	CIRC	this work
349.03	0.377	0.05	1.826	0.05	EBU	this work
351.15	0.313	0.1	1.859	0.10	DDIST	this work
353.5	0.539	0.05	2.192	0.03	EBU	this work
353.5	0.581	0.05	2.233	0.05	CIRC	this work
363.87	0.721	0.05	2.825	0.05	EBU	this work
363.87	0.807	0.1	2.911	0.10	CIRC	this work
370.86	0.75	0.05	3.142	0.03	EBU	this work
372.28	0.716	0.05	3.165	0.03	CIRC	this work

^a CIRC, circulation equilibrium still; DEWT, dew temperature measurement; DDIST, differential distillation; EBU, ebulliometry; RDIST, Rayleigh distillation; TENS, tensimetry; TRANS, transpiration method.

^b Calculated from the Redlich-Kister fit of p - x data and p_1^s values reported in the cited source. ^c Calculated from air-water partition coefficients reported in the cited source and p_1^s from Table 2 ($\gamma_1^\infty = K_{aw}RT/(p_1^s v_2^s)$). ^d Calculated from air-water partition coefficients reported in the cited source ($K_H = K_{aw}RT/v_2^s$). ^e Calculated from limiting activity coefficient reported in the cited source and p_1^s from Table 2 ($K_H = \gamma_1^\infty p_1^s$). ^f Calculated from relative volatility in highly dilute solutions reported in the cited source (eq 5). ^g Calculated from relative volatility in highly dilute solutions reported in the cited source (eq 3).

Table 4. Values of Limiting Partial Molar Excess Enthalpies $\bar{H}_1^{E,\infty}$ and Hydration Enthalpies $\Delta_{\text{hyd}}H_1^\infty$ of N-Methylated (C1 and C2) Fatty Acid Amides (1) in Water (2) Used in Simultaneous Fits by Equation 6

T	$\bar{H}_1^{E,\infty}$	$s(\bar{H}_1^{E,\infty})$	$\Delta_{\text{hyd}}H_1^\infty$	$s(\Delta_{\text{hyd}}H_1^\infty)$	technique ^a	ref
K	$\text{kJ}\cdot\text{mol}^{-1}$	$\text{kJ}\cdot\text{mol}^{-1}$	$\text{kJ}\cdot\text{mol}^{-1}$	$\text{kJ}\cdot\text{mol}^{-1}$		
NMF						
298.15	-7.14	0.02	-63.39 ^b	0.09	BATCH	31
298.15	-7.08	0.02	-63.33 ^b	0.09	BATCH	32
298.15	-7.11	0.02	-63.36 ^b	0.09	BATCH	33
NMA						
304.01	-12.59	0.05			BATCH	34
307.07	-12.34	0.05			BATCH	34
298.15			-73.45 ^c	0.3	BATCH	34
298.15			-74.87 ^c	0.5	BATCH	35
298.15			-73.80 ^c	0.3	BATCH	31
298.15			-73.71 ^c	0.3	BATCH	36
DMF						
298.15	-15.22	0.02	-62.10 ^b	0.5	BATCH	31
298.15	-15.27	0.01	-62.16 ^b	0.5	BATCH	33
298.15	-15.3	0.2	-62.19 ^b	0.5	FLOW	37
DMA						
298.15	-21.41	0.01	-71.64 ^b	0.2	BATCH	31
298.15	-21.46	0.04	-71.69 ^b	0.2	BATCH	33
298.15	-21.42	0.01	-71.65 ^b	0.2	BATCH	38

^a BATCH, batch dissolution calorimetry; FLOW, flow mixing calorimetry. ^b $\Delta_{\text{hyd}}H_1^\infty = \bar{H}_1^{E,\infty} - \Delta_{\text{vap}}H_1$, vaporization enthalpy $\Delta_{\text{vap}}H_1$ taken from ref 20. ^c Calculated from dissolution enthalpy $\Delta_{\text{sol}}H_1^\infty$ of the solid solute reported in the cited source and its sublimation enthalpy $\Delta_{\text{subl}}H_1$ taken from ref 39 ($\Delta_{\text{hyd}}H_1^\infty = \Delta_{\text{sol}}H_1^\infty - \Delta_{\text{subl}}H_1$).

so that its composition remains effectively unchanged. Samples of the collected distillate and the batch solution are then analyzed by a suitable analytical method. Provided the analytical response is proportional to the solute concentration, the ratio of the responses for the distillate and the batch solution, A_1^G/A_1^L , gives directly α_{12}^∞ , in the same way as in the case of the CIRC method (eq 2).

In the present implementation of DDIST, the stripping by an inert gas at isothermal conditions was used instead of heating to conduct the distillation as an equilibrium process. A schematic diagram of our experimental setup is shown in Figure 1. The equilibrium cell is an all-glass jacketed device destined to hold about 300 mL of the solution under study. The cell was thermostatted by an electronic water-circulating bath (Medingen U6CP) to better than ± 0.02 K. The inert gas at a constant flow rate maintained by a digital flow controller (Aalborg DFC 2600) was introduced into the solution through a fine porosity fritted glass tip which dispersed it into small-diameter bubbles. The solution was mixed with an efficient magnetic stirrer. Vigorous mixing extended the path and residence time of the bubbles in the solution whereby promoting rapid equilibration. The saturated gas exited the cell via a glass transfer tube which was electrically heated to a temperature approximately 30 K higher than that of the cell to prevent condensation. The vapors were then quantitatively captured in a dry ice trap at the end of the tubing. Typically, about 3 mL of distillate was collected. With the nitrogen flow rates set between (4 and 12) $\text{mL}\cdot\text{min}^{-1}$, the distillation experiments for the present systems took from (12 to 34) h, depending on the system and temperature. Samples of the original solution and of the distillate were analyzed by gas chromatography precisely in the same manner as in the case of the CIRC method.

Results of Measurements. Air-water partitioning data measured in this work for four lower N-methylated amides (NMF, NMA, DMF, and DMA) are reported in Table 1. Besides

Table 5. Values of Limiting Partial Molar Excess Heat Capacities $\bar{C}_{p,1}^{E,\infty}$ and Hydration Heat Capacities $\Delta_{\text{hyd}}C_{p,1}^{\infty}$ of N-Methylated (C1 and C2) Fatty Acid Amides (1) in Water (2) Used in Simultaneous Fits by Equation 6

T K	$\bar{C}_{p,1}^{E,\infty}$ ^a J·K ⁻¹ ·mol ⁻¹	$s(\bar{C}_{p,1}^{E,\infty})$ J·K ⁻¹ ·mol ⁻¹	$\Delta_{\text{hyd}}C_{p,1}^{\infty}$ ^b J·K ⁻¹ ·mol ⁻¹	$s(\Delta_{\text{hyd}}C_{p,1}^{\infty})$ J·K ⁻¹ ·mol ⁻¹	technique ^c	ref ^d
			NMF			
298.15	40.2	2	99.2	2	DROP	32, 32, 40
298.15	39.2	5	97.2	5	SCAN	41, 42, 40
298.15	37.0	2	98.2	2	ADIAB	43, 43, 40
			NMA			
298.15	106.6 ^e	6	164.1	5	DROP	32, 32, 44
298.15	101.6 ^e	6	164.1	5	SCAN	41, 32, 44
303.15			166.1	4	SCAN	41, -, 44
313.15			167.9	4	SCAN	41, -, 44
323.15			169.8	4	SCAN	41, -, 44
333.15			171.6	4	SCAN	41, -, 44
343.15			172.7	4	SCAN	41, -, 44
353.15			174.4	4	SCAN	41, -, 44
363.15			175.3	4	SCAN	41, -, 44
373.15			176.2	4	SCAN	41, -, 44
298.15	102.6 ^e	4	160.1	5	SCAN	45, 32, 44
303.15			163.1	4	SCAN	45, -, 44
313.15			165.9	4	SCAN	45, -, 44
323.15			167.8	4	SCAN	45, -, 44
333.15			169.6	4	SCAN	45, -, 44
343.15			171.5	4	SCAN	45, -, 44
353.15			172.4	4	SCAN	45, -, 44
363.15			172.3	4	SCAN	45, -, 44
373.15			176.2	4	SCAN	45, -, 44
			DMF			
298.15	76.9	3			FLOW	46, 46, -
283.15	70	5			SCAN	47, 42, -
293.15	77	5			SCAN	47, 42, -
298.15	80	5			SCAN	47, 42, -
303.15	82	5	135	4	SCAN	47, 42, 44
313.15	87	5	139	4	SCAN	47, 42, 44
323.15	92	5	142	4	SCAN	47, 42, 44
333.15	96	5	146	4	SCAN	47, 42, 44
343.15	99	5	148	4	SCAN	47, 42, 44
353.15	101	5	150	4	SCAN	47, 42, 44
363.15	103	5	152	4	SCAN	47, 42, 44
373.15	105	5	153	4	SCAN	47, 42, 44
			DMA			
298.15	119	10	184	14	ADIAB	48, 48, 16
278.15	109	6			SCAN	47, 42, -
283.15	112	5			SCAN	47, 42, -
288.15	115	5			SCAN	47, 42, -
293.15	118	5			SCAN	47, 42, -
298.15	121	2	186	10	SCAN	47, 42, 16

^a Calculated from partial molar heat capacity at infinite dilution $\bar{C}_{p,1}^{\infty}$ and molar heat capacity of pure liquid solute $C_{p,1}^{L,*}(\bar{C}_{p,1}^{E,\infty} = \bar{C}_{p,1}^{\infty} - C_{p,1}^{L,*})$.

^b Calculated from partial molar heat capacity at infinite dilution $\bar{C}_{p,1}^{\infty}$ and ideal gas molar heat capacity of pure solute $C_{p,1}^{G,0}$ ($\Delta_{\text{hyd}}C_{p,1}^{\infty} = \bar{C}_{p,1}^{\infty} - C_{p,1}^{G,0}$).

^c ADIAB, adiabatic calorimetry; DROP, drop calorimetry; FLOW, flow calorimetry; SCAN, scanning calorimetry. ^d Data sources of $C_{p,1}^{\infty}$, $C_{p,1}^{L,*}$, and $C_{p,1}^{G,0}$, respectively. ^e Subcooled liquid $C_{p,1}^{L,*}$ estimated from a homologous trend by Sköld et al.³²

the limiting relative volatility α_{12}^{∞} , the results are given here also in the form of other closely related quantities, namely, Henry's law constant K_H (defined as the limiting ratio of the solute liquid phase fugacity and its mole fraction), air–water partition coefficient K_{aw} (defined as the limiting ratio of the solute equilibrium concentrations in air and water), and limiting activity coefficient γ_1^{∞} , which were calculated considering the ideal behavior of the gas phase as follows

$$K_H = \alpha_{12}^{\infty} p_2^s \quad (3)$$

$$K_{\text{aw}} = \alpha_{12}^{\infty} p_2^s v_2^L / (RT) \quad (4)$$

$$\gamma_1^{\infty} = \alpha_{12}^{\infty} p_2^s / p_1^s \quad (5)$$

In eqs 3 to 5, p_1^s and p_2^s are the vapor pressures of amide and water, respectively, and v_2^L is the molar volume of pure liquid water. Due attention was paid to the selection of sufficiently accurate amide vapor pressure data to minimize the resulting

uncertainty of γ_1^{∞} values. Literature information on vapor pressures of the four amides was gathered and critically evaluated. The selected vapor pressure data are given in Table 2 as parameters of the Wagner equation or the Riedel–Planck equation. These vapor pressure data are considered reliable in the temperature range of our air–water partitioning measurements, but at lower temperatures, where the amide vapor pressures are low, one must count with their substantially enhanced uncertainty. We noted that even the recently reported $p_1^s(T)$ data for DMF¹⁷ and DMA¹⁸ exhibit at 298.15 K a severe inconsistency with calorimetrically determined vaporization enthalpy,²⁰ the difference of the calculated value and the calorimetric one being about 11 kJ·mol⁻¹ and -7 kJ·mol⁻¹, respectively. Water vapor pressure was calculated from the accurate reference equation of Wagner and Pruss.¹⁹ As estimated by error propagation, considering contributions from all possible sources of errors, the combined standard uncertainty of the

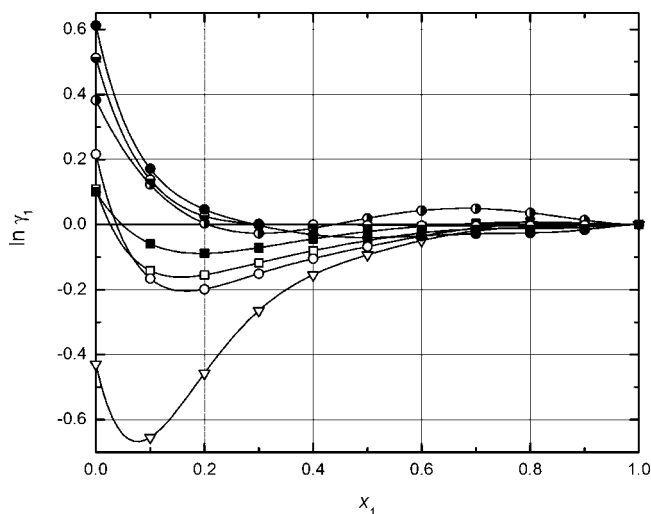


Figure 2. Activity coefficient $\ln \gamma_1$ of amide (1) in water (2) as a function of mole fraction x_1 . Obtained from the Redlich–Kister correlation of isothermal pTx_1 data: \square -, NMF, 303.15 K, ref 9; \blacksquare -, NMF, 313.15 K, ref 8; \circ -, NMA, 313.15 K, ref 10; \bullet -, NMA, 333.15 K, ref 7; \ominus -, NMA, 353.15 K, ref 7; \bullet -, NMA, 373.15 K, ref 7; ∇ -, DMA, 313.15 K, ref 11.

results given in Table 1 is typically from (3 to 5) % and never exceeds 10 %.

Data Correlation. While reasonably accurate measurements of the amide air–water partitioning can be done at rather elevated temperatures (> 333 K), at near-ambient temperatures such determinations are hardly feasible because severe experimental difficulties arise from the extremely low amide concentrations that prevail in the equilibrium vapor above the highly dilute aqueous solution. To establish a reliable temperature dependence of the air–water partitioning characteristics allowing extrapolation to lower (near-ambient) temperatures, we combined the present air–water partitioning data and some other relevant VLE measurements from the literature with existing calorimetric data on respective derivative thermal properties and processed the entire information by a thermodynamically consistent treatment. The strategy and procedure we followed are essentially the same as those we applied previously and proved to work efficiently for a variety of other aqueous solutes.^{21–24}

Basically, for each solute, the experimental data on its dissolution or hydration Gibbs energy G_1 ($\ln \gamma_1^\infty$ or $\ln K_H$), respective enthalpy H_1 ($\bar{H}_1^{E,\infty}$ or $\Delta_{\text{hyd}}H_1^\infty$), and heat capacity $C_{p,1}$ ($\bar{C}_{p,1}^{E,\infty}$ or $\Delta_{\text{hyd}}C_{p,1}^\infty$) were correlated simultaneously by the following equation

$$G_1 = A + B/\tau + C \ln \tau + D\tau \quad (6)$$

Giving

$$H_1 = RT_0(B - C\tau - D\tau^2) \text{ and } C_{p,1} = -R(C + 2D\tau)$$

where $\tau = T/T_0$ and $T_0 = 298.15$ K. If all four adjustable parameters, A , B , C , and D , are used, eq 6 implies that the $C_{p,1}$ is linearly dependent on temperature. All four parameters could be considered only if sufficient experimental information on the temperature dependence of $C_{p,1}$ is available; otherwise, the three-parameter form of eq 6 (i.e., $D = 0$), implying constant $C_{p,1}$, had to be used. The adjustable parameters were calculated from a weighted least-squares method. The minimized objective function was as follows

$$S = \sum_{i=1}^{n_G} [G_{1,i}(\text{exptl}) - G_{1,i}(\text{calcd})]^2 / s^2(G_{1,i}) + \sum_{i=1}^{n_H} [H_{1,i}(\text{exptl}) - H_{1,i}(\text{calcd})]^2 / s^2(H_{1,i}) + \sum_{i=1}^{n_C} [C_{p,1,i}(\text{exptl}) - C_{p,1,i}(\text{calcd})]^2 / s^2(C_{p,1,i}) \quad (7)$$

with data being weighted according to their standard uncertainties $s^2(G_{1,i})$, $s^2(H_{1,i})$, $s^2(C_{p,1,i})$.

For estimation and assignment of these data uncertainties, we followed the policy and procedure which have been described in detail and extensively applied in our previous studies.^{21–24} In principle, the assigned uncertainties comprise contributions of errors from all possible sources, both random and systematic. As a result, they should account for any scatter and/or disparity of existing data, which in other words means that the statistical coherence of all data within their uncertainty bounds should be obtained. The goodness-of-fit test for the standard deviation of fit was used to indicate the coherence. Statistically reasonable sizes of individual residuals and their distribution among the three properties were considered as additional constraints.

Database Used. Experimental data used in the fitting are listed in Tables 3, 4, and 5. They represent a comprehensive collection that was gathered through a careful literature search and extended by the present air–water partitioning measurements. The quality of collected data is not at all uniform, the fact being reflected by the combined standard uncertainties provided. Table footnotes indicate the source form of data if different from that adopted for the processing and give details on their transformation to a common basis.

As seen from Table 3, dilute range VLE measurements of acceptable quality were presented in the literature only for DMF; for the other three amides, the literature results are few and turn out to be substantially in error. In contrast, accurate full range VLE data are available for these systems (static measurements of Zielkiewicz^{8–11} for NMF, NMA, DMA, and dynamic measurements of Manczinger and Kortüm⁷ for DMA), and hence γ_1^∞ values could be estimated by extrapolation. Although generally not recommendable, under the present circumstances (lack of other data, experimental difficulties, and enhanced level of uncertainty of direct air–water partitioning determinations), this approach of obtaining γ_1^∞ data may be well justified. To that end, we fitted the full range VLE data (pTx) by a multiparameter Redlich–Kister expansion using the Barker method. This processing was done with p_1^s values measured on the pure amide samples used in the pTx determinations, to avoid any distortion due to possible incompatibility of pTx and p_1^s data. Special care was also taken to avoid any over- or underfitting. An adequate number of adjustable parameters was selected considering appropriate statistical criteria (F-test, randomness of residuals). Figure 2 shows the $\gamma_1(x_1)$ courses which resulted from the data reduction. In spite of being remarkably complicated, these courses are for the three amides very similar and exhibit a quite regular temperature variation. It appears that the complicated $\gamma_1(x_1)$ dependences reflect a very complex structure of amide–water solutions^{3,4} rather than that they are a correlation artifact. Nevertheless, to be on the safe side, the combined standard uncertainties we give for the extrapolated γ_1^∞ values are more than double those calculated from the variance–covariance matrix of the fitted parameters.

As seen from Tables 4 and 5, the calorimetric information on amide dissolution and hydration is relatively abundant, but

Table 6. Parameters of Equation 6^a Obtained by Simultaneous Fit of G_1 , H_1 , and $C_{p,1}$ Data, Number of Respective Underlying Data Points n_G , n_H , and n_C , Weighted Root-Mean-Square Deviations (WRMSD) of Individual Properties, and Overall Standard Deviation of Fit s^b

solute	A	B	C	D	$n_G/n_H/n_C$	WRMSD ^c			s^b	
						G_1	H_1	$C_{p,1}$		
$G_1 = \ln \gamma_1^\infty$, $H_1 = \bar{H}_1^{E,\infty}$, $C_{p,1} = \bar{C}_{p,1}^{E,\infty}$										
N-methylformamide	7.53452	-7.52028	-4.65167	-	6/3/3	0.63	1.16	0.66	1.24	
N-methylacetamide	17.7536	-17.8231	-12.4870	-	8/2/3	1.49	0.67	0.38	1.37	
N,N-dimethylformamide	15.1467	-8.54144	4.72765	-7.11309	27/3/12	0.85	1.29	0.47	0.84	
N,N-dimethylacetamide	22.4622	-14.9699	1.7858	-8.11614	16/3/6	1.39	0.76	0.26	1.23	
$G_1 = \ln(K_H/\text{kPa})$, $H_1 = \Delta_{\text{hyd}}H_1^\infty$, $C_{p,1} = \Delta_{\text{hyd}}C_{p,1}^\infty$										
N-methylformamide	34.0606	-37.3482	-11.7869	-	6/3/3	1.31	0.27	0.41	1.11	
N-methylacetamide	45.42529	-46.6756	-14.0990	-2.81867	8/4/19	1.81	1.22	0.42	1.11	
N,N-dimethylformamide	40.2666	-36.7266	-7.0191	-4.62646	27/3/8	1.27	0.10	0.27	1.14	
N,N-dimethylacetamide	48.6627	-50.7278	-21.8138	-	16/3/2	1.36	0.16	0.38	1.29	

^a Recommended temperature dependence for limiting activity coefficient and Henry's law constant from (293 to 373) K. ^b $s = [S_{\text{min}}/(n-p)]^{1/2}$; S is given by eq 7, p is the number of adjustable parameters. ^c WRMSD = $(1/n_Y \sum_{i=1}^{n_Y} [Y_i(\text{exptl}) - Y_i(\text{calcd})]^2/s^2(Y_i))^{1/2}$, $Y = G_1, H_1, C_{p,1}$.

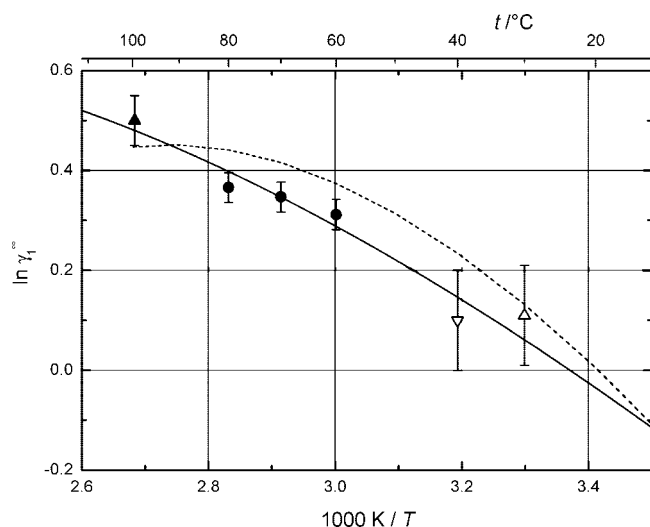


Figure 3. Limiting activity coefficient $\ln \gamma_1^\infty$ of NMF (1) in water (2) as a function of temperature. Experimental values are from Table 3: ∇ , ref 9; Δ , ref 8; \bullet , this work (DDIST); \blacktriangle , this work (CSM). The solid line indicates the recommended temperature dependence obtained by simultaneous fit of γ_1^∞ , $\bar{H}_1^{E,\infty}$, and $\bar{C}_{p,1}^{E,\infty}$ data by eq 6, and the dashed line is the prediction by the modified UNIFAC (Dortmund).

the enthalpic data are generally limited to ambient temperature. Concerning heat capacity data, this limitation is encountered for NMF. For other amides, the infinite dilution partial molar heat capacity data were measured as a function of temperature, yet in some cases $\bar{C}_{p,1}^{E,\infty}$ or $\Delta_{\text{hyd}}C_{p,1}^\infty$ could not be determined because respective pure solute heat capacities $C_{p,1}^{L,*}$ or $C_{p,1}^{G,0}$ were not available at corresponding temperatures.

Results of Correlations and Discussion

The simultaneous correlation of air–water partitioning data with respective calorimetric information enabled us to discriminate between existing data and to establish thermodynamically consistent temperature dependences of the air–water partition characteristics. For each of the aqueous amides studied, the calculated parameters of eq 6 are given, together with the standard deviations of the fit and other fit characteristics, in Table 6. Experimental limiting activity coefficients and their temperature dependences established by the simultaneous fits are plotted in the van't Hoff coordinates in Figures 3 to 6. As seen, most data agree mutually quite well, but there are also some data deviating grossly (>0.2 in $\ln \gamma_1^\infty$) from the fits. According to our evaluation policy, such data were not strictly rejected but rather labeled with a larger uncertainty, which reduced appropriately their statistical weight in the treatment.

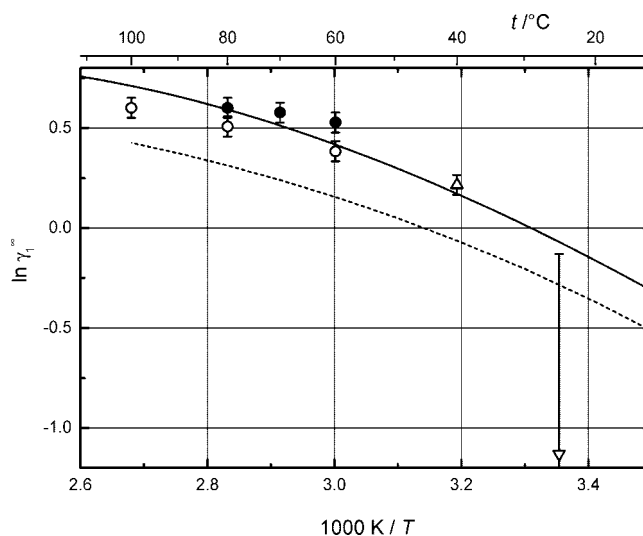


Figure 4. Limiting activity coefficient $\ln \gamma_1^\infty$ of NMA (1) in water (2) as a function of temperature. Experimental values are from Table 3: \circ , ref 7; Δ , ref 10; ∇ , ref 25; \bullet , this work (DDIST). The solid line indicates the recommended temperature dependence obtained by simultaneous fit of γ_1^∞ , $\bar{H}_1^{E,\infty}$, and $\bar{C}_{p,1}^{E,\infty}$ data by eq 6, and the dashed line is the prediction by the modified UNIFAC (Dortmund).

The grossly deviating points, which are undoubtedly subject to large errors, correspond to (i) room-temperature transpiration measurements carried out for NMA and DMA by Wolfenden,²⁵ (γ_1^∞ too low), (ii) Rayleigh distillation measurements of Shalygin et al.³⁰ in the range from (314 to 373) K for DMA (γ_1^∞ too high and contradicting calorimetric data), and (iii) ebulliometric measurements at (333 and 343) K of Bergmann and Eckert²⁶ for DMF (γ_1^∞ too high and contradicting calorimetric data). For all other determinations, the correlation deviations $\delta \ln \gamma_1^\infty$ are reasonable, mostly within 0.1. One can note a good mutual agreement between the present measurements carried out by the various techniques (EBU, DDIST, and CIRC) as well as their reasonable accord with existing literature data, namely, with those derived from accurate full composition range pT_x measurements of Zielkiewicz^{8–11} at lower temperatures. Analogous figures for $K_H(T)$ (not shown) have much smaller resolution than those for $\gamma_1^\infty(T)$, but the correlations are of similar quality and indicate the same outliers. Note that this fact excludes uncertainty in pure amide vapor pressure data as a possible cause of the gross deviations and identifies the respective air–water partitioning measurements alone to be greatly in error.

Compared to the air–water partitioning measurements, the calorimetric determinations of dissolution and hydration thermal properties of the amides studied appear to be considerably less

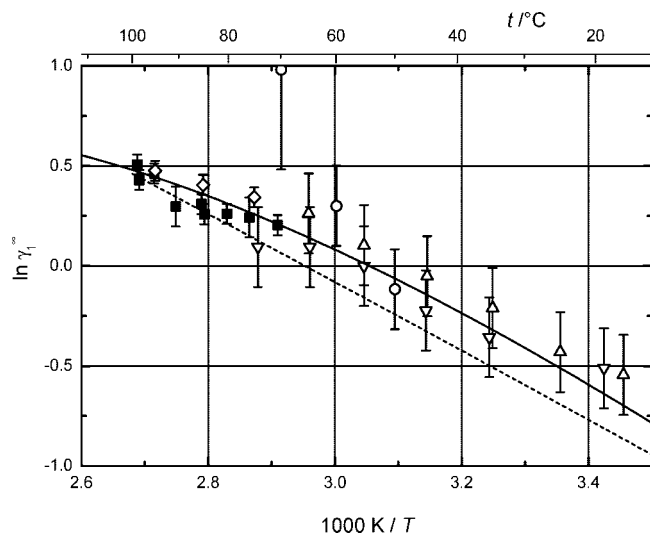


Figure 5. Limiting activity coefficient $\ln \gamma_1^\infty$ of DMF (1) in water (2) as a function of temperature. Experimental values are from Table 3: O, ref 26; Δ , ref 27; ∇ , ref 28; \diamond , ref 29; \blacksquare , this work (EBU). The solid line indicates the recommended temperature dependence obtained by simultaneous fit of γ_1^∞ , $\bar{H}_1^{E,\infty}$, and $\bar{C}_{p,1}^{E,\infty}$ data by eq 6, and the dashed line is the prediction by the modified UNIFAC (Dortmund).

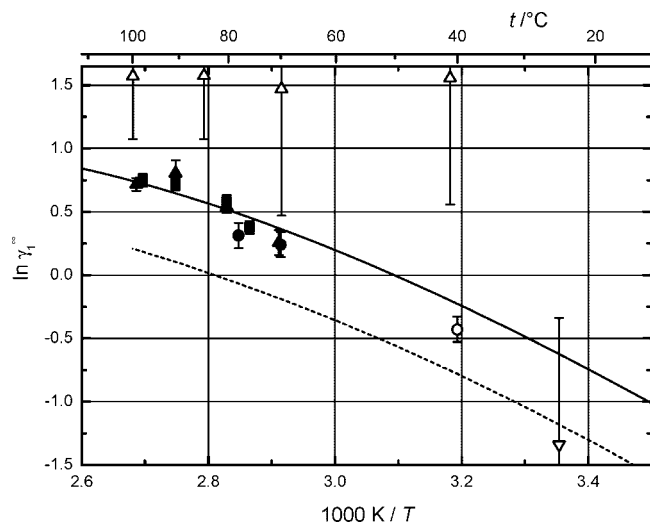


Figure 6. Limiting activity coefficient $\ln \gamma_1^\infty$ of DMA (1) in water (2) as a function of temperature. Experimental values are from Table 3: O, ref 30; Δ , ref 11; ∇ , ref 25; \blacksquare , this work (EBU); \bullet , this work (DDIST); \blacktriangle , this work (CSM). The solid line indicates the recommended temperature dependence obtained by simultaneous fit of γ_1^∞ , $\bar{H}_1^{E,\infty}$, and $\bar{C}_{p,1}^{E,\infty}$ data by eq 6, and the dashed line is the prediction by the modified UNIFAC (Dortmund).

scattered, the results from different sources showing almost perfect agreement. Both enthalpies and heat capacities were thus fitted very closely (see WRMSDs of H_1 and $C_{p,1}$ in Table 6), and these data also almost exclusively determined the course of temperature dependence of air–water partitioning characteristics. Being efficiently stabilized by the calorimetric information, the simultaneous correlations we carried out allow quite reliable extrapolation of amide air–water partitioning characteristics toward lower temperatures where direct air–water partitioning measurements and pure amide vapor pressure data are missing or uncertain.

Since eq 6 with parameters from Table 6 yields for available data a thermodynamically consistent description of superior quality, we consider it to establish the recommended temperature dependence of γ_1^∞ and K_H as well as the related thermal

Table 7. Recommended Values of Limiting Activity Coefficients γ_1^∞ , Henry's Law Constants K_H , and Air Water Partitioning Coefficients K_{aw}

T/K	γ_1^∞	K_H/kPa	$10^6 K_{aw}$
NMF			
298.15	1.02	0.037	0.27
323.15	1.25	0.260	1.79
348.15	1.45	1.28	8.42
373.15	1.62	4.83	30.4
NMA			
298.15	0.93 ^a	0.017	0.13
323.15	1.36	0.160	1.14
348.15	1.74	0.976	6.59
373.15	2.04	4.22	27.4
DMF			
298.15	0.60	0.34	2.5
323.15	0.94	2.23	15.4
348.15	1.29	10.2	67.1
373.15	1.61	35.0	221
DMA			
298.15	0.54	0.13	0.92
323.15	1.00	1.11	7.64
348.15	1.56	6.29	41.3
373.15	2.10	25.4	160

^a Refers to hypothetical subcooled liquid standard state. NMA melting temperature $T_m = 303.71$ K (ref 34).

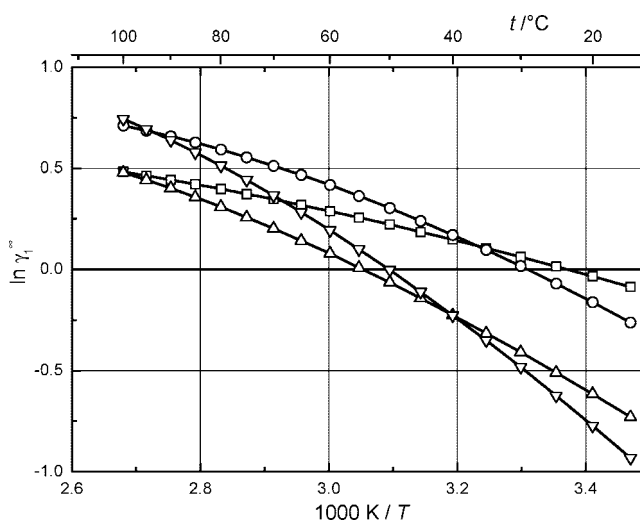


Figure 7. Recommended temperature dependence for limiting activity coefficients γ_1^∞ of N-methylated (C1 and C2) fatty acid amides: \square , NMF; \circ , NMA; \triangle , DMF; ∇ , DMA.

properties in the range from 373 K down to ambient temperature. Note however that for NMA the values of γ_1^∞ and other dissolution properties calculated from eq 6 at temperatures below its melting point (303.71 K)³⁴ refer to the hypothetical subcooled liquid standard state. For a quick reference and illustration, recommended values of γ_1^∞ , K_H , and K_{aw} at several representative temperatures are listed in Table 7. The recommended K_{aw} values (dimensionless Henry's law constants) were readily inferred from those of K_H through factorizing by the term $v_2^\infty/(RT)$. The relative combined standard uncertainty (68 % confidence level) of the recommended values, as estimated by the error propagation considering the stability of the fits (parameter variance–covariance matrix) and systematic sources of error (e.g., uncertainty of pure solute vapor pressure data), is approximately 3 % in the range from (333 to 373) K, increasing with decreasing temperature to about 5 % at 323 K and 10 % at 298 K.

As seen from Table 7 and Figure 7, the limiting activity coefficients of the studied amides exhibit at subambient and

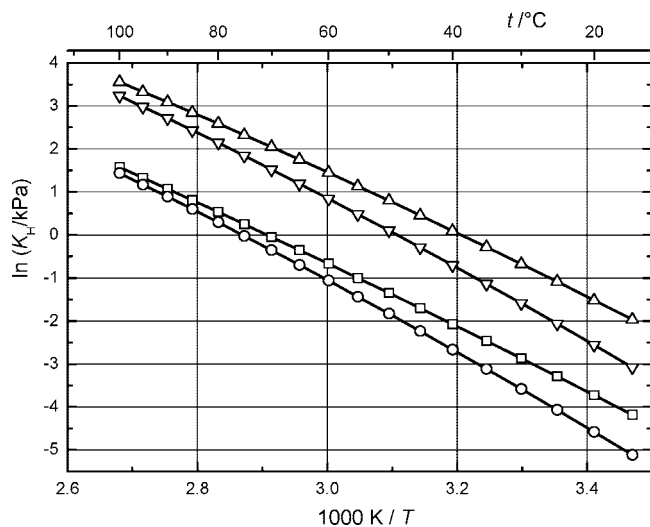


Figure 8. Recommended temperature dependence for Henry's law constants K_H of N-methylated (C1 and C2) fatty acid amides: \square , NMF; \circ , NMA; ∇ , DMA; Δ , DMF; \circ , DMA.

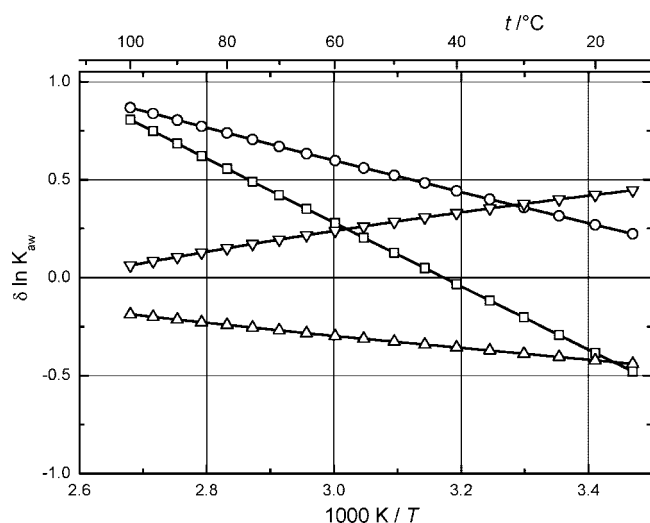


Figure 9. Deviation $\delta \ln K_{aw} = \ln K_{aw}(\text{predicted}) - \ln K_{aw}(\text{recommended})$ as a function of temperature for the group contribution method of Cabani et al.: \square , NMF; \circ , NMA; ∇ , DMA; Δ , DMF; \circ , DMA.

ambient temperatures values lower than unity, but these negative deviations convert more or less rapidly to positive ones with increasing temperature. In accord with positive $\bar{C}_{p,1}^{E,\infty}$ values, the van't Hoff plots exhibit negative curvature, but moderate extrapolation of the recommended $\gamma_1^\infty(T)$ dependences above the normal boiling temperature of water, which can be considered still reliable, shows no maximum to occur up to 400 K. The relatively small deviations of γ_1^∞ from unity result from a close compensation of large enthalpy (favorable) and entropy (unfavorable) terms, whose delicate balance changes with temperature. This thermodynamic phenomenology reflects a complicated interplay of hydrophilic and hydrophobic molecular interactions in which amide–water and water–water hydrogen bonding are the major ones.

In Figure 8, the recommended temperature dependences of Henry's law constants are displayed in van't Hoff coordinates. As one can expect, the Henry's law constants in the temperature range considered increase monotonously and rapidly with temperature. The volatility of the amide solutes from their infinitely dilute aqueous solutions increases in the sequence $\text{NMA} < \text{NMF} < \text{DMA} < \text{DMF}$ spanning approximately over an order of magnitude; however, the differences between the

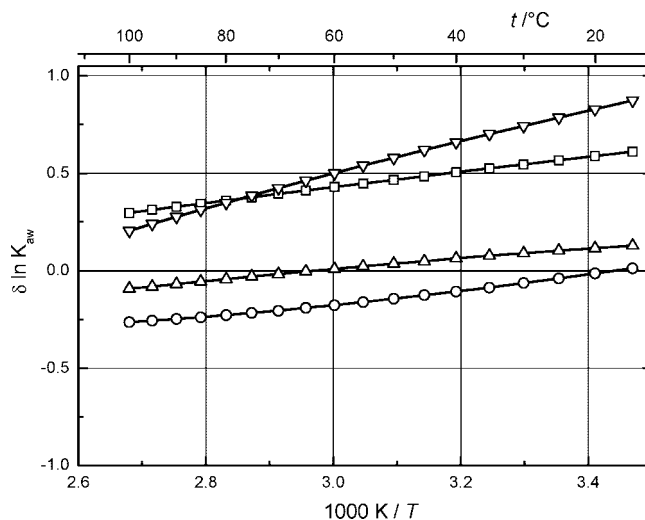


Figure 10. Deviation $\delta \ln K_{aw} = \ln K_{aw}(\text{predicted}) - \ln K_{aw}(\text{recommended})$ as a function of temperature for the LFER correlation (L) of Abraham:⁵⁰ \square , NMF; \circ , NMA; ∇ , DMA; Δ , DMF; \circ , DMA.

formamides and acetamides with the same degree of methylation diminish with rising temperature, and their volatilities appear to converge at temperatures slightly above the normal boiling point of water.

Performance of Predictive Approaches. As a part of this work, the performance of three predictive approaches, namely, the modified UNIFAC, the method of Cabani et al.,⁴⁹ and the LFER correlation of Abraham,⁵⁰ to estimate the air–water partitioning of the amides was also examined. The leading group contribution method, modified UNIFAC (Dortmund), was applied with the latest parameter values published in the open literature (fourth⁵¹ and fifth revision⁵²) to predict $\gamma_1^\infty(T)$ dependences. The results of the prediction are shown in Figures 3 to 6. The method of Cabani et al. and the LFER correlation of Abraham were applied to predict the $K_{aw}(T)$ dependences which were constructed using the predicted $K_{aw}(298.15 \text{ K})$, $\Delta_{\text{hyd}}H_1^\infty(298.15 \text{ K})$, and $\Delta_{\text{hyd}}C_{p,1}^\infty(298.15 \text{ K})$ values. Because the group contributions to $K_{aw}(298.15 \text{ K})$ for monosubstituted (CONH) and disubstituted (CON) amides in the method of Cabani et al. are not available, we adjusted them to the $K_{aw}(298.15 \text{ K})$ recommended values given in Table 7. Concerning the Abraham LFER correlation, both its forms, L and V, were applied, but results are given only for the L form because of its considerably better performance for the amides studied. The results for the methods of Cabani and Abraham are given in the form of deviation plots in Figures 9 and 10, respectively.

The predictions by the modified UNIFAC are, except for DMA, very good, reflecting for all amides studied in this work correct temperature trends. To value the results one should take into account that in the modified UNIFAC method each of the amides considered is described using a specific amide functional group (groups HCONR, CONR, DMF, and CONR₂). The Cabani method is seen to perform significantly worse; here, the adoption of a uniform value of either CONH contribution for NMF and NMA or CON for DMF and DMA appears not to be supported by the recommended $K_{aw}(298.15 \text{ K})$ values, and also large errors in the predicted $\Delta_{\text{hyd}}H_1^\infty(298.15 \text{ K})$ values are encountered (note large slopes of the deviation plot especially for NMF and NMA). Similarly to the modified UNIFAC, the Abraham LFER correlation works well for NMA and DMF in the entire temperature range considered. The results for the other two amides, especially for DMA, are however rather unsatisfactory.

Conclusion

The recommended temperature dependences of limiting activity coefficient and Henry's law constant established in this work for N-methylated (C1 and C2) fatty acid amides in water improve our knowledge of gas-liquid partitioning of these aqueous solutes. The present results provide reasonably accurate thermodynamically consistent information which can be used for further development of empirical predictive tools and theoretical models of these complex solutions having great importance for biochemistry, process engineering, and environmental protection.

Literature Cited

- Rizzo, R. C.; Jorgensen, W. L. OPLS All-Atom Model for Amines: Resolution of the Amine Hydration Problem. *J. Am. Chem. Soc.* **1999**, *121*, 4827–4836.
- Graziano, G. Hydration Thermodynamics of N-Methylacetamide. *J. Phys. Soc. Jpn.* **2000**, *69*, 3720–3725.
- Zielkiewicz, J. Preferential solvation of N-methylformamide, N,N-dimethylformamide and N-methylacetamide by water and alcohols in the binary and ternary mixtures. *Phys. Chem. Chem. Phys.* **2000**, *2*, 2925–2923.
- Lei, Y.; Li, H.; Pan, H.; Han, S. Structures and Hydrogen Bonding Analysis of N,N-Dimethylformamide and N,N-Dimethylformamide-Water Mixtures by Molecular Dynamics Simulations. *J. Phys. Chem. A* **2003**, *107*, 1574–1583.
- Aparicio-Martinez, S.; Balbuena, P. B. On the properties of aqueous amide solutions through classical molecular dynamics simulations. *Mol. Simul.* **2007**, *33*, 925–938.
- Panuszko, A.; Gojlo, E.; Zielkiewicz, J.; Smiechowski, M.; Krakowiak, J. Hydration of Simple Amides. FTIR Spectra of HDO and Theoretical Studies. *J. Phys. Chem. B* **2008**, *112*, 2483–2493.
- Manczinger, J.; Kortüm, G. Thermodynamische Mischungseffekte im System Wasser(1)/N-Methylacetamid(2). *Z. Phys. Chem. (Neue Folge)* **1975**, *95*, 177–186.
- Zielkiewicz, J. (Vapour+liquid) equilibria in (N-methylformamide+methanol+water) at the temperature 313.15 K. *J. Chem. Thermodyn.* **1996**, *28*, 887–894.
- Zielkiewicz, J. Excess molar volumes and excess Gibbs energies in N-methylformamide+water, or +methanol, or +ethanol at the temperature 303.15 K. *J. Chem. Eng. Data* **1998**, *43*, 650–652.
- Zielkiewicz, J. (Vapour + liquid) equilibrium measurements and correlation of the ternary mixture (N-methylacetamide + methanol + water) at the temperature 313.15 K. *J. Chem. Thermodyn.* **1999**, *31*, 819–825.
- Zielkiewicz, J. (Vapour + liquid) equilibrium in (N,N-dimethylacetamide + methanol + water) at the temperature 313.15 K. *J. Chem. Thermodyn.* **2003**, *35*, 1993–2003.
- Dohnal, V.; Novotná, M. Infinite-dilution activity coefficients by comparative ebulliometry: the mixtures of freon 112 with oxygenated solvents and hydrocarbons. *Fluid Phase Equilib.* **1985**, *23*, 303–313.
- Dohnal, V.; Novotná, M. Infinite-dilution activity coefficients by comparative ebulliometry: a model of ebulliometer and the experimental equipment and procedure. *Collect. Czech. Chem. Commun.* **1986**, *51*, 1393–1402.
- Dohnal, V.; Fenclová, D. Air-Water Partitioning and Aqueous Solubility of Phenols. *J. Chem. Eng. Data* **1995**, *40*, 478–483.
- Andon, R. J. L.; Cox, J. D.; Herington, E. F. G. Phase Relationships in the Pyridine Series. Part V. The Thermodynamic Properties of Dilute Solutions of Pyridine Bases in Water at 25 and 40 C. *J. Chem. Soc.* **1954**, *50*, 3188–3196.
- Evaluated Standard Thermophysical Property Values, DIPPR 801 Database*; Design Institute for Physical Properties; Sponsored by AIChE, 1995.
- Cui, X.; Chen, G.; Han, X. Experimental Vapor Pressure Data and a Vapor Pressure Equation for N,N-Dimethylformamide. *J. Chem. Eng. Data* **2006**, *51*, 1860–1861.
- Nasirzadeh, K.; Neueder, R.; Kunz, W. Vapor Pressures of Propylene Carbonate and N,N-Dimethylacetamide. *J. Chem. Eng. Data* **2005**, *50*, 26–28.
- Wagner, W.; Pruss, A. The IAPWS Formulation 1995 for the thermodynamic properties of ordinary water substance for general and scientific use. *J. Phys. Chem. Ref. Data* **2002**, *31*, 387–535.
- Barone, G.; Castronuovo, G.; Della Gatta, G.; Elia, V.; Iannone, A. Enthalpies of vaporization of seven alkylamides. *Fluid Phase Equilib.* **1985**, *21*, 157–164.
- Dohnal, V.; Fenclová, D.; Vrbka, P. Temperature Dependences of Limiting Activity Coefficients, Henry's Law Constants, and Derivative Infinite Dilution Properties of Lower (C1–C5) 1-Alkanols in Water. Critical Compilation, Correlation, and Recommended Data. *J. Phys. Chem. Ref. Data* **2006**, *35*, 1621–1651.
- Bernauer, M.; Dohnal, V.; Roux, A. H.; Roux-Desgranges, G.; Majer, V. Temperature Dependences of Limiting Activity Coefficients and Henry's Law Constants for Nitrobenzene, Aniline, and Cyclohexylamine in Water. *J. Chem. Eng. Data* **2006**, *51*, 1678–1685.
- Ondo, D.; Dohnal, V. Temperature Dependence of Limiting Activity Coefficients and Henry's Law Constant of Cyclic and Open-Chain Ethers in Water. *Fluid Phase Equilib.* **2007**, *262*, 121–136.
- Fenclová, D.; Dohnal, V.; Vrbka, P.; Laštovka, V. Temperature Dependences of Limiting Activity Coefficients, Henry's Law Constants, and Related Infinite Dilution Properties of Branched (C3 and C4) Alkanols in Water. Measurement, Critical Compilation, Correlation and Recommended Data. *J. Chem. Eng. Data* **2007**, *52*, 989–1002.
- Wolfenden, R. Interaction of the peptide bond with solvent water: a vapor phase analysis. *Biochemistry* **1978**, *17*, 201–204.
- Bergmann, D. L.; Eckert, C. A. Measurement of limiting activity coefficients for aqueous systems by differential ebulliometry. *Fluid Phase Equilib.* **1991**, *63*, 141–150.
- Trampe, D. B.; Eckert, C. A. A Dew Point Technique for Limiting Activity Coefficients in Nonionic Solutions. *AIChE J.* **1993**, *39*, 1045–1050.
- Suleiman, D.; Eckert, C. A. Limiting Activity Coefficients of Diols in Water by a Dew Point Technique. *J. Chem. Eng. Data* **1994**, *39*, 692–696.
- Proust, P. C.; Meyer, E. A.; Jaque, Z. L. Infinite-dilution activity coefficients for systems with N,N-dimethylformamide using a differential ebulliometry experimental technique. *Lat. Am. Appl. Res.* **1995**, *25*, 181–184.
- Shalygin, V. A.; Shitikov, V. V.; Smirnova, G. E. Glubokaja Ochistka Dimetilacetamida. *Vysokochistye Veshchestva* **1988**, *6*, 132–136.
- Stimson, R. E.; Schrier, E. E. Calorimetric Investigation of Salt-Amide Interactions in Aqueous Solution. *J. Chem. Eng. Data* **1974**, *19*, 354–358.
- Sköld, R.; Suurkuusk, J.; Wadsö, I. Thermochemistry of solutions of biochemical model compounds 7. Aqueous solutions of some amides, t-butanol and pentanol. *J. Chem. Thermodyn.* **1976**, *8*, 1075–1080.
- Rouw, A. C.; Somsen, G. Solvation and Hydrophobic Hydration of Alkyl-substituted Ureas and Amides in N,N-Dimethylformamide + Water Mixtures. *J. Chem. Soc., Faraday Trans. 1* **1982**, *78*, 3397–3408.
- Kreis, R. W.; Wood, R. H. Enthalpy of fusion and cryoscopic constant of N-methylacetamide. *J. Chem. Thermodyn.* **1969**, *1*, 523–526.
- Kresheck, G. C.; Klotz, I. M. Thermodynamics of transfer of amides from an apolar to an aqueous solution. *Biochemistry* **1969**, *8*, 8–12.
- Ojelund, G.; Sköld, R.; Wadsö, I. Thermochemistry of solutions of biochemical model compounds 5. Transfer of N-alkylamides from water to non-aqueous media. *J. Chem. Thermodyn.* **1976**, *8*, 45–54.
- Dohnal, V.; Roux, A. H.; Hynek, V. Limiting partial molar excess enthalpies by flow calorimetry: some organic solvents in water. *J. Solution Chem.* **1994**, *23*, 889–900.
- Batov, D. V.; Manin, N. G.; Zaichikov, A. M. Enthalpy characteristics and state of N,N-disubstituted amides of formic and acetic acids in water-formamide mixtures. *Russ. J. Gen. Chem.* **2001**, *71*, 853–859.
- Starzewski, P.; Wadso, I.; Zielkiewicz, W. Enthalpies of vaporization of some N-alkylamides at 298.15 K. *J. Chem. Thermodyn.* **1984**, *16*, 331–334.
- TRC Thermodynamic Tables. Hydrocarbons*; Thermodynamics Research Center, Texas Engineering Experiment Station, The Texas A&M University System: College Station, TX, 1994.
- Makhatadze, G. I.; Lopez, M. M.; Privalov, P. L. Heat capacities of protein functional groups. *Biophys. Chem.* **1997**, *64*, 93–101.
- Zábranský, M.; Růžička, V.; Majer, V.; Domalski, E. S. Heat Capacity of Liquids: Volume I: Critical Review and Recommended Values. *J. Phys. Chem. Ref. Data, Monogr.* **1996**, *6*, 1–810.
- Visser, C.; Pel, P.; Somsen, G. Volumes and heat capacities of water and N-methylformamide in mixtures of these solvents. *J. Solution Chem.* **1977**, *6*, 571–580.
- CDATA: Database of Thermodynamic and Transport Properties for Chemistry and Engineering*; Department of Physical Chemistry, Institute of Chemical Technology, Distributed by FIZ Chemie GmbH: Berlin, Prague, 1991.
- Swenson, D. M.; Ziemer, S. P.; Blodgett, M. B.; Jones, J. S.; Wooley, E. M. Apparent molar volumes and apparent molar heat capacities of aqueous N-acetyl-d-glucosamine at temperatures from 278.15 to 368.15 K and of aqueous N-methylacetamide at temperatures from 278.15 to 393.15 K at the pressure 0.35 MPa. *J. Chem. Thermodyn.* **2006**, *38*, 1523–1531.
- Visser, C.; Perron, G.; Desnoyers, J.; Heuvelsland, M. J.; Somsen, G. Volumes and Heat Capacities of Mixtures of N,N-Dimethylformamide and Water at 298.15 K. *J. Chem. Eng. Data* **1977**, *22*, 74–79.
- Origlia, M. L.; Patterson, B. A.; Wooley, E. M. Apparent molar volumes and apparent molar heat capacities of aqueous solutions of

- N,N-dimethylformamide and N,N-dimethylacetamide at temperatures from 278.15 to 393.15 K and at the pressure 0.35 MPa. *J. Chem. Thermodyn.* **2001**, *33*, 917–927.
- (48) Visser, C.; Heuvelsland, M. J.; Dunn, A. L.; Somsen, G. Some Properties of Binary Aqueous Liquid Mixtures. Apparent Molar Volumes and Heat Capacities at 298.15 K Over the Whole Mole Fraction Range. *J. Chem. Soc., Faraday Trans. 1* **1978**, *74*, 1159–1169.
- (49) Cabani, S.; Gianni, P.; Mollica, V.; Lepori, L. Group Contributions to the Thermodynamic Properties of Non-Ionic Organic Solutes in Dilute Aqueous Solution. *J. Solution Chem.* **1981**, *10*, 563–595.
- (50) Abraham, M. H.; Acree, W. E. Prediction of gas to water partition coefficients from 273 to 373 K using predicted enthalpies and heat capacities of hydration. *Fluid Phase Equilib.* **2007**, *262*, 97–110.
- (51) Gmehling, J.; Witting, R.; Lohmann, J.; Joh, R. A Modified UNIFAC (Dortmund) Model. 4. Revision and Extension. *Ind. Eng. Chem. Res.* **2002**, *41*, 1678–1688.
- (52) Jakob, A.; Grensemann, H.; Lohmann, J.; Gmehling, J. Further Development of Modified UNIFAC (Dortmund): Revision and Extension 5. *Ind. Eng. Chem. Res.* **2006**, *45*, 7924–7933.

Received for review July 4, 2008. Accepted September 11, 2008. The support of the Ministry of Education of the Czech Republic (Grant MSM 604 613 7307) is acknowledged.

JE800517R